Title

Loss of function of a rice TPR-domain RNA-binding protein confers broad-spectrum disease resistance

Journal

Proceedings of the National Academy of Sciences of the United States of America, 115(12)

ISSN

0027-8424

Authors

Zhou, Xiaogang
Liao, Haicheng
Chern, Mawsheng
et al.

Publication Date

2018-03-20

DOI

10.1073/pnas.1705927115

Peer reviewed

Loss of function of a rice TPR-domain RNA-binding protein confers broad-spectrum disease resistance

Xiaogang Zhou[a,b,c,d,1], Haicheng Liao[a,b,c,1], Mawsheng Chern[e,f,1], Junjie Yin[a,b,c,1], Yufei Chen[a,b,c], Jianping Wang[a,b,c], Xiaobo Zhu[a,b,c], Zhixiong Chen[a,b,c], Can Yuan[a,b,c], Wen Zhao[a,b,c], Jing Wang[a,b,c], Weitao Li[a,b,c], Min He[a,b,c], Bingtian Ma[a,b,c], Jichun Wang[a,b,c], Peng Qin[a,b,c], Weilan Chen[a,b,c], Yuping Wang[a,b,c], Jiali Liu[a,b,c], Yangwen Qian[g], Wenming Wang[a,b,c], Xianjun Wu[a,b,c], Ping Li[a,b,c], Lihuang Zhu[h,i], Shigui Li[a,b,c], Pamela C. Ronald[e,f], and Xuewei Chen[a,b,c,2]

[a]Key Laboratory of Major Crop Diseases, Sichuan Agricultural University, Wenjiang, Chengdu, Sichuan 611130, China; [b]State Key Laboratory of Hybrid Rice, Sichuan Agricultural University, Wenjiang, Chengdu, Sichuan 611130, China; [c]Collaborative Innovation Center for Hybrid Rice in Yangtze River Basin, Rice Research Institute, Sichuan Agricultural University, Wenjiang, Chengdu, Sichuan 611130, China; [d]Key Laboratory for Aging and Regenerative Medicine, Department of Pharmacology, School of Pharmacy, Southwest Medical University, Luzhou, Sichuan 646000, China; [e]Department of Plant Pathology, University of California, Davis, CA 95616; [f]The Genome Center, University of California, Davis, CA 95616; [g]Biogle Genome Editing Center, Changzhou, Jiangsu 213125, China; [h]State Key Laboratory of Plant Genomics, Chinese Academy of Sciences, Beijing 100101, China; and [i]National Center for Plant Gene Research, Institute of Genetics and Developmental Biology, Chinese Academy of Sciences, Beijing 100101, China

Edited by Xinnian Dong, Duke University, Durham, NC, and approved January 9, 2018 (received for review April 13, 2017)

Crops carrying broad-spectrum resistance loci provide an effective strategy for controlling infectious disease because these loci typically confer resistance to diverse races of a pathogen or even multiple species of pathogens. Despite their importance, only a few crop broad-spectrum resistance loci have been reported. Here, we report the identification and characterization of the rice *bsr-k1* (broad-spectrum resistance Kitaake-1) mutant, which confers broad-spectrum resistance against *Magnaporthe oryzae* and *Xanthomonas oryzae* pv *oryzae* with no major penalty on key agronomic traits. Map-based cloning reveals that *Bsr-k1* encodes a tetratricopeptide repeats (TPRs)-containing protein, which binds to mRNAs of multiple *OsPAL* (*OsPAL1–7*) genes and promotes their turnover. Loss of function of the *Bsr-k1* gene leads to accumulation of *OsPAL1–7* mRNAs in the *bsr-k1* mutant. Furthermore, overexpression of *OsPAL1* in wild-type rice TP309 confers resistance to *M. oryzae*, supporting the role of *OsPAL1*. Our discovery of the *bsr-k1* allele constitutes a significant conceptual advancement and provides a valuable tool for breeding broad-spectrum resistant rice.

blast disease | broad-spectrum resistance | innate immunity | TPR protein | rice

Plant disease causes devastating yield losses in crop production, threatening global food security (1, 2). Repeated over-application of pesticides to control plant diseases has polluted many environments around the globe (3, 4). Crop genetic improvement for resistance is the most economical and environmentally friendly approach to preventing disease outbreaks (3, 4). Although many resistance (*R*) genes conferring race-specific resistance have been deployed in plant breeding, their resistance often remains effective for only a few years, presumably due to strong selection pressure for evolution of virulent races (5, 6). In contrast, the broad-spectrum resistance controlled by multiple genes or quantitative trait loci (QTLs) is often durable and therefore more effective for disease management (5, 6).

To date, nine plant genes conferring broad-spectrum resistance have been isolated: *Arabidopsis RPW8.2* (7), rice *Xa21*, *STV11*, *pi21*, *Pigm*, and *bsr-d1* (8–12), wheat *Lr34* and *Yr36* (13, 14), and barley *mlo* (15). Only a few of these genes have their molecular mechanisms of action elucidated. *Arabidopsis* RPW8.2 is specifically targeted to the plant extrahaustorial membrane adjacent to fungal haustorium and activates the salicylic acid (SA)-dependent defense response, leading to broad-spectrum resistance against diverse races of powdery mildew (16). Rice *Xa21* encoding a receptor kinase phosphorylates downstream genes to trigger a series of defense responses, bringing about broad-spectrum resistance to *Xanthomonas oryzae* pv *oryzae* (*Xoo*) (17). Rice *STV11* encodes a sulfotransferase catalyzing the conversion of SA to sulfonated SA, conferring broad-spectrum resistance to rice stripe virus (9). Rice *bsr-d1* reduces the expression of H_2O_2-degrading enzymes through the binding of a repressive MYB transcription factor (MYBS1) to the *bsr-d1* promoter, generating broad-spectrum resistance to *Magnaporthe oryzae* (12). Wheat *Yr36* encodes a kinase-START protein, which phosphorylates the thylakoid-associated ascorbate peroxidase in chloroplast, resulting in broad-spectrum resistance to diverse races of stripe rust (18).

In some cases, close linkage to undesirable agricultural traits has hindered the use of broad-spectrum resistance genes to effectively control diseases of elite cultivars. For example, wheat *Lr34* lines produce less grain than lines without *Lr34* (19). The barley recessive *mlo* mutant displays early senescence-like leaf chlorosis (20). The rice *pi21* gene is tightly linked with a gene causing inferior grain quality (10). Thus, there is a need to identify novel genes conferring broad-spectrum resistance for integration into crop genomes without penalizing major superior agricultural traits.

Here we report the rice *bsr-k1* (broad-spectrum resistance Kitaake-1) mutant that displays broad-spectrum resistance against *M. oryzae* and *Xoo* and maintains major agronomic traits. Map-based cloning reveals that *Bsr-k1* encodes a tetratricopeptide repeats (TPRs)-containing protein. Disruption of *Bsr-k1* enhances

Significance

Crops carrying broad-spectrum resistance loci provide an effective strategy for controlling infectious disease. Despite their importance, few broad-spectrum resistance loci have been reported, and the underlying mechanisms controlling the trait remain largely unknown. This report describes the identification of a gene, called "*bsr-k1*," conferring broad-spectrum resistance and demonstrates that the encoded protein regulates immunity-related genes. Loss of function of BSR-K1 in rice leads to enhanced broad-spectrum resistance to two serious rice diseases with no major penalty on yield. This report provides insights into broad-spectrum resistance and offers an efficient strategy to breeding durably resistant rice.

Author contributions: X. Zhou and X.C. designed research; X. Zhou, H.L., J.Y., Y.C., Jianping Wang, and Y.Q. performed research; X. Zhou, M.C., X. Zhu, Z.C., C.Y., W.Z., Jing Wang, W.L., M.H., B.M., Jichun Wang, P.Q., W.C., Y.W., J.L., W.W., X.W., P.L., L.Z., S.L., and X.C. analyzed data; and X. Zhou, M.C., P.C.R., and X.C. wrote the paper.

The authors declare no conflict of interest.

This article is a PNAS Direct Submission.

See Commentary on page 2859.

[1]X. Zhou, H.L., M.C., and J.Y. contributed equally to this work.

[2]To whom correspondence should be addressed. Email: xwchen88@163.com.

This article contains supporting information online at www.pnas.org/lookup/suppl/doi:10.1073/pnas.1705927115/-/DCSupplemental.

Published online February 5, 2018.

resistance to diverse isolates of *M. oryzae* and *Xoo*. The BSR-K1 protein binds to mRNAs of the defense-related *OsPAL* genes, promoting their turnover. Loss of function of BSR-K1 decreases mRNA turnover, resulting in *OsPAL* mRNA accumulation in the *bsr-k1* mutant. Collectively, our study reveals the mechanism by which BSR-K1 regulates the immune response and provides a tool for breeding rice with broad-spectrum resistance.

Results

The Rice *bsr-k1* Mutant Confers Enhanced Resistance Against Diverse Races of *M. oryzae* and *Xoo*. To identify genes involved in rice blast resistance, we generated a mutant population containing ~50,000 lines in the model rice Kitaake cultivar through ethylmethane sulfonate (EMS)-mediated mutagenesis. We then inoculated these lines with mixed spores derived from seven Kitaake-compatible *M. oryzae* isolates (ZB25, Zhong1, Tetep, 99-20-2, 97-27-2, 0755-1-1, and ZE-1) in the field. We obtained five mutant lines showing enhanced disease resistance compared with wild-type Kitaake. Of these, the *bsr-k1* mutant exhibits significantly smaller lesion length and fewer lesions than Kitaake (Fig. 1 *A* and *B*). We validated the smaller lesion size and lower fungal biomass accumulation in *bsr-k1* (Fig. S1*A*) using a punch inoculation method (21). We then tested the seven Kitaake-compatible blast isolates individually in field inoculation. We found that the lesion numbers were dramatically reduced in *bsr-k1* with all isolates (Fig. 1*C*). For example, *bsr-k1* yields 1.6 ± 0.8 lesions, while Kitaake has 4.4 ± 1.2, when inoculated with isolate ZB25 (Fig. 1*C*). To assess if *bsr-k1* enhances resistance to other pathogens, we inoculated *bsr-k1* and Kitaake with 10 *Xoo* isolates (P2–P7, P9, P10, 8248, and *Xoo*-4) that are commonly used to test for broad-spectrum resistance to rice bacterial blight (22). We found that *bsr-k1* confers enhanced resistance to all 10 *Xoo* isolates (Fig. 1*D*).

Because the immune response in plants is usually accompanied by the induction of defense-related genes, such as *OsPR1a* (*Os07g0129200*), *OsPR10* (*Os12g0555200*), and *PBZ1* (*Os12g0555500*) (21), we measured the expression of these three genes in *bsr-k1* and Kitaake plants using qRT-PCR. We observed that expression levels of these three defense-related genes are moderately elevated (two- to threefold) in *bsr-k1* compared with Kitaake plants (Fig. 1*E*). Together, these results demonstrate that the *bsr-k1* mutant confers broad-spectrum resistance to *M. oryzae* and *Xoo* compared with Kitaake.

The *bsr-k1* Mutant Maintains Key Agronomic Traits. We next monitored several key agronomic traits in the *bsr-k1* mutant to assess its application potential in rice breeding. We examined *bsr-k1* and Kitaake plants for their yield-related traits (in Lingshui, Hainan, China), including thousand-grain weight, grain length and width, panicle length, grain numbers per panicle, grain yield per plant, and other traits, including tiller numbers and heading date. Few differences were observed between *bsr-k1* and Kitaake (Fig. 1*F* and Fig. S1*B*). For example, the thousand-grain weights of *bsr-k1* (28.52 ± 0.38 g) and Kitaake (28.89 ± 0.23 g) are similar, and the average heading dates of *bsr-k1* (55.9 ± 1.1 d) and Kitaake (56.1 ± 1.4 d) are comparable (Fig. 1*F*). These results suggest that the *bsr-k1* allele does not penalize major agronomic traits.

Map-Based Cloning Identified the Causative Mutation of *bsr-k1*. To identify the *bsr-k1* locus, we generated three F_2 populations by crossing the resistant *bsr-k1* mutant with susceptible cultivars Kitaake and Joden, separately. Genetic analyses showed that the *bsr-k1* resistance phenotype was controlled by a single recessive locus (Dataset S1). We selected 995 F_2 plants from Joden × *bsr-k1* that exhibited high-level resistance against blast isolate 99-20-2 and determined the resistance level in each F_3 progeny (Dataset S1). By using 88 resistant F_2 individuals, we first mapped the *bsr-k1* locus to a 1.37-Mb interval between markers

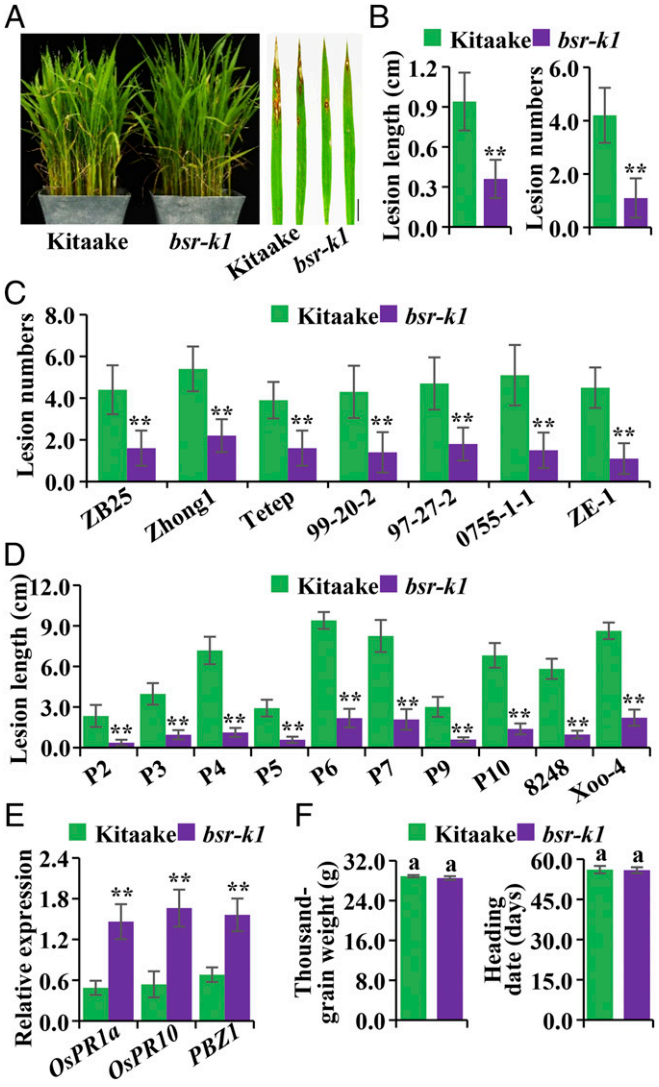

Fig. 1. Phenotypic characterization of the *bsr-k1* allele. (*A*) Field inoculation of *bsr-k1* and wild-type Kitaake plants. Shown are photographs of representative plants and leaves taken 10 d postinoculation (dpi) with spore mixtures of seven Kitaake-compatible blast isolates. (Scale bar: 1 cm.) (*B*) Lesion lengths and numbers (mean ± SD, $n > 30$) after inoculation with seven Kitaake-compatible blast isolates. (*C*) Lesion numbers (mean ± SD, $n > 30$) after inoculation with seven individual blast isolates (names are given under bars). (*D*) Lesion lengths measured 14 dpi with 10 individual *Xoo* isolates (names are given below the bars). (*E*) Comparison of defense gene expression levels (mean ± SEM, $n = 3$) in *bsr-k1* and Kitaake. This experiment was repeated twice with similar results. (*F*) Comparison of thousand-grain weights and heading dates. Error bars represent mean ± SD ($n > 30$). The same letter above bars indicates same statistical group ($P > 0.05$, Tukey's multiple-comparison test). Asterisks indicate statistical significance (**$P \leq 0.01$, *t* test).

RM25789 and RM333 on chromosome 10 (Fig. 2*A*). Analysis of another 907 resistant F_2 individuals located it to a 50-kb region between insertion–deletion markers ID13 and ID16 (Fig. 2*A*) containing 11 predicted genes (Dataset S2). We then sequenced the genomic DNA sample bulked from 25 resistant BC_2F_4 individuals and Kitaake control DNA separately using whole-genome resequencing. In the 50-kb region, we identified a single nucleotide substitution (G2447A) located at the 3′ splice site of intron 8 in gene *Os10g0548200* (Fig. 2*B* and Fig. S2*A*). Sequencing of cDNA confirms that *bsr-k1* produces a variant *Os10g0548200* transcript with a 71-bp insertion derived from intron 8, causing a premature termination (Fig. S2 *B–D*).

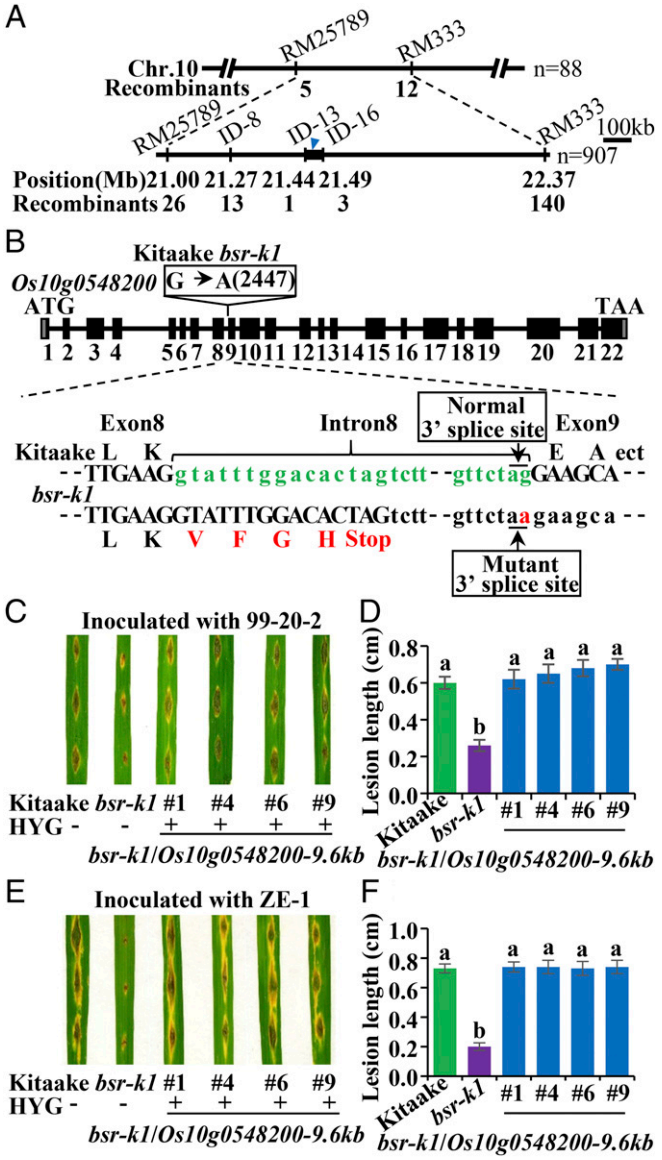

Fig. 2. Positional cloning of *bsr-k1*. (*A*) Fine mapping of the *bsr-k1* locus. The molecular markers and the number of recombinants are indicated. (*B*) Structure of the *Bsr-k1* gene and the mutation in *bsr-k1*. Filled boxes indicate exons (numbered 1–22) of *Os10g0548200*. The change from G to A in *Os10g0548200* in *bsr-k1* is indicated in the open box above exon 9. Nucleotide sequences between exon 8 and exon 9 in Kitaake and *bsr-k1* with deduced amino acid sequences are shown below. The substitution in *bsr-k1* (in red) abolishes the 3′ splice site of intron 8, resulting in premature termination of translation. (*C–F*) Blast-resistance test of *Bsr-k1*–complemented lines. (*C* and *E*) Photographs of four independent representative lines at 7 dpi with blast fungal isolates 99-20-2 (*C*) and ZE-1 (*E*). (*D* and *F*) Lesion lengths (mean ± SD, $n > 10$) of the complemented lines, *bsr-k1*, and Kitaake inoculated with blast isolates 99-20-2 (*D*) and ZE-1 (*F*). Different letters above bars indicate significant differences ($P < 0.05$, Tukey's test). This punch inoculation was repeated twice with similar results.

To confirm that the *bsr-k1* resistance phenotype was caused by this mutation, we introduced the *Os10g0548200* genomic DNA (9.6 kb) into *bsr-k1*. All 15 independent, complemented lines carrying wild-type *Os10g0548200* reverted to susceptibility to all seven blast isolates. We chose four of the complemented lines for further investigation. Punch inoculation with *M. oryzae* isolates 99-20-2 and ZE-1 revealed that the lesions in these complemented lines were similar in size to those in Kitaake whereas the *bsr-k1* mutant was resistant (Fig. 2 *C–F*). These complemented lines also show susceptibility to *Xoo* similar to Kitaake (Fig. S3*A*). We then generated two independent *Os10g0548200*-KO lines in Kitaake using the CRISPR/Cas9 approach (Fig. S3 *B* and *C*) and performed inoculation with *M. oryzae* and *Xoo*. These KO lines show enhanced resistance, displaying smaller lesion size, less *M. oryzae* DNA accumulation, and lower *Xoo* population than Kitaake (Fig. S3 *D–F*). In addition, plants overexpressing *Os10g0548200* show much larger lesions compared with Kitaake (Fig. S3 *G–J*). Taken together, these results demonstrate that the

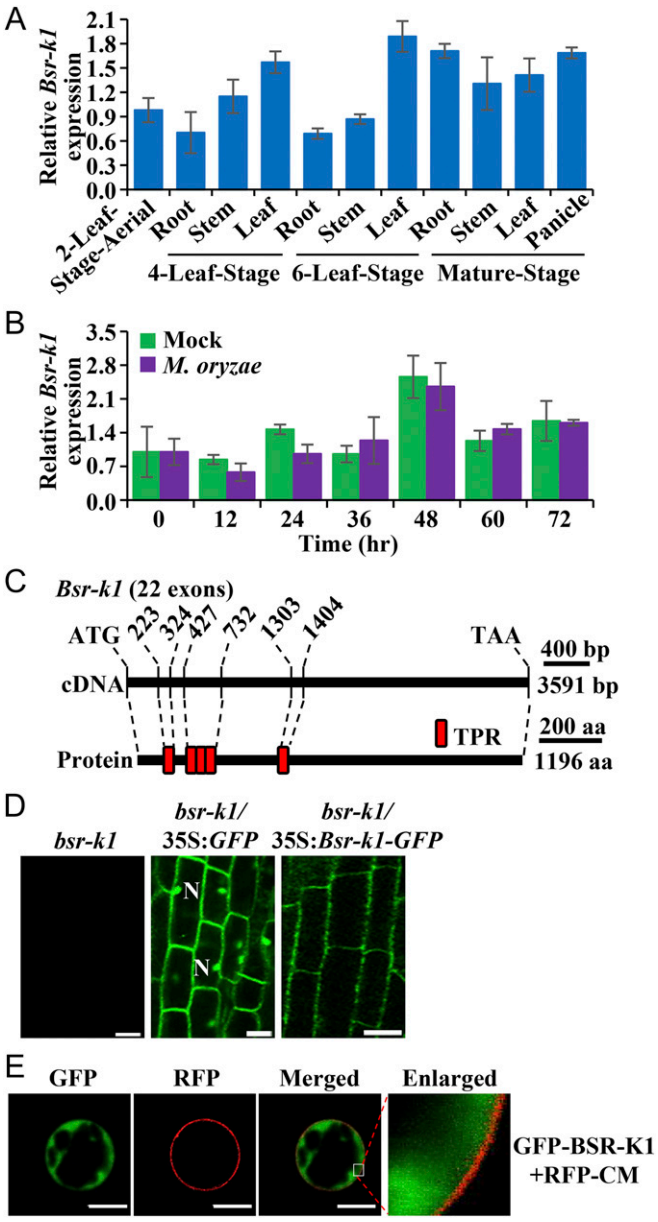

Fig. 3. Expression pattern of *Bsr-k1* and subcellular localization of BSR-K1. (*A*) *Bsr-k1* RNA expression pattern. (*B*) *Bsr-k1* RNA levels (mean ± SEM, $n = 3$) post *M. oryzae* or mock inoculation. This experiment was repeated twice with similar results. (*C*) Schematic structure of BSR-K1. The nucleotide numbers above the cDNA indicate the locations of the five TPR motifs. The TPR motifs are represented as red boxes. (*D*) Subcellular localization of BSR-K1 in rice root tips. Photographs of representative root tips were taken under confocal laser-scanning microscopy. N, nucleus. (Scale bars: 20 μm.) (*E*) Subcellular localization of BSR-K1 in rice protoplasts. The white square in the merged image is enlarged and shown at the right. CM, mCherry-cytomembrane. (Scale bars: 5 μm.)

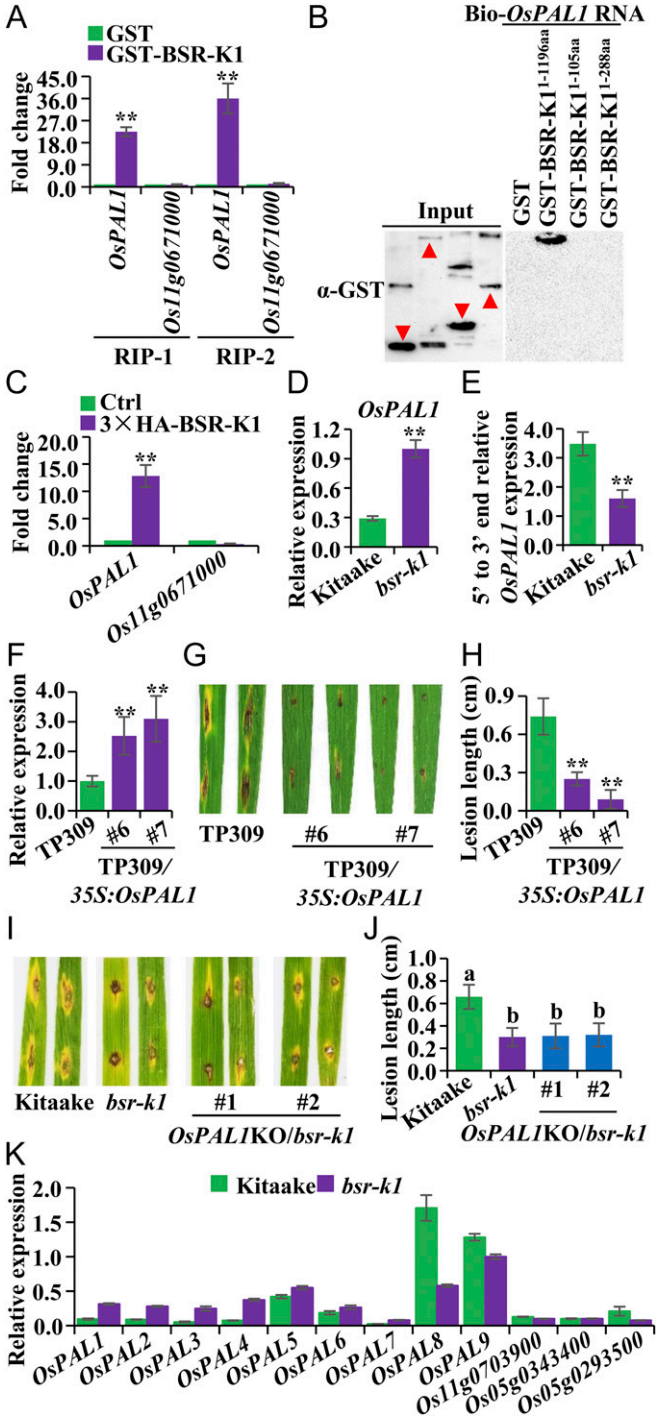

Fig. 4. BSR-K1 binds to *OsPAL1* mRNA and regulates its turnover. (*A*) qRT-PCR verification of *OsPAL1* mRNA enrichment in two independent RIP experiments (Dataset S3*C*). The enrichment was calculated as the fold change of RNA abundance comparing GST-BSR-K1 pulldown with GST pulldown. The *Os11g0671000* gene was used as a negative control. (*B*) RNA pull-down assays with biotinylated *OsPAL1* RNA. BSR-K1$^{1–1,196aa}$, full-length BSR-K1; BSR-K1$^{1–105aa}$, the truncated BSR-K1 protein in the *Bsr-k1*KO plant; BSR-K1$^{1–288aa}$, the truncated BSR-K1 protein in the *bsr-k1* mutant. The red triangles in input indicate bands of target proteins. This experiment was repeated twice with similar results. (*C*) Enrichment of *OsPAL1* RNA in *3×HA-Bsr-k1* plants as detected by qRT-PCR. The enrichment was calculated as the fold change in the abundance of RNA immunoprecipitated in *3×HA-Bsr-k1* plants compared with Kitaake. *Os11g0671000* was used as a negative control (Ctrl). (*D*) *OsPAL1* mRNA levels in *bsr-k1* and Kitaake. (*E*) *OsPAL1* mRNA turnover rates (mean ± SEM, $n = 3$) in *bsr-k1* and Kitaake. This experiment was repeated twice with similar results. (*F*) qRT-PCR detection of *OsPAL1* mRNA (mean ± SEM, $n = 3$) in two overexpression lines. (*G*) Punch inoculation of wild-type TP309 and two independent *OsPAL1* overexpression lines. Two leaves each of TP309, TP309/*35S:OsPAL1*-#6, and TP309/*35S:OsPAL1*-#7 are shown. (*H*) Lesion lengths (mean ± SD, $n > 10$) of TP309, TP309/35S:*OsPAL1*-#6, and TP309/*35S:OsPAL1*-#7 inoculated with the blast isolate Zhong1. (*I*) Punch inoculation of *OsPAL1*KO/*bsr-k1* plants. Two leaves each of Kitaake, *bsr-k1*, *OsPAL1*KO/*bsr-k1*-#1, and *OsPAL1*KO/*bsr-k1*-#2 are shown. (*J*) Lesion lengths (mean ± SD, $n > 10$) of Kitaake, *bsr-k1*, *OsPAL1*KO/*bsr-k1*-#1, and *OsPAL1*KO/*bsr-k1*-#2 inoculated with the blast isolate Zhong1. The same letter above bars indicates the same statistical group ($P > 0.05$, Tukey's multiple-comparison test). (*K*) Expression levels (mean ± SEM, $n = 3$) of *OsPAL* genes and other defense-related genes detected by RIP-seq (Dataset S3*C*) in *bsr-k1* mutant and Kitaake. This experiment was repeated twice with similar results. $^{**}P \leq 0.01$, *t* test.

Os10g0548200 gene hosts the *bsr-k1* mutation where a single nucleotide change results in enhanced resistance.

***Bsr-K1* Is Constitutively Expressed and Encodes a Cytoplasm-Localized TRP.** To investigate the expression pattern of *Bsr-k1*, we sampled roots, stems, leaves, and panicles of Kitaake plants at the four- and six-leaf and mature stages and performed qRT-PCR to measure RNA levels. We found that *Bsr-k1* is expressed across all stages and in various tissues but predominantly in leaves (Fig. 3*A*). To determine whether *Bsr-k1* is induced by *M. oryzae* infection, we assessed the *Bsr-k1* RNA level in Kitaake before and after *M. oryzae* inoculation and found that *Bsr-k1* RNA levels remain similar in mock- and *M. oryzae*-inoculated samples (Fig. 3*B*). These results suggest that *Bsr-k1* is constitutively expressed in rice and is not induced by *M. oryzae* infection.

The *Bsr-k1* ORF encodes a protein of 1,196 amino acids containing five tandem TPRs (Fig. 3*C*). To determine the subcellular localization of the BSR-K1 protein, we used confocal laser-scanning microscopy to analyze the roots of plants carrying a functional GFP-tagged BSR-K1 protein, which complemented the *bsr-k1* mutant (Fig. S3 *G–J*), and found that its GFP signal is excluded from the nucleus, whereas the GFP protein alone is present in both the cytoplasm and nucleus (Fig. 3*D*). We validated this result by expressing the GFP-BSR-K1 protein in *Nicotiana benthamiana* (Fig. S4) and in rice protoplasts, where the GFP-BSR-K1 protein was detected only in the cytoplasm but not in the nucleus or cytomembrane (visualized by the mCherry-cytomembrane marker, RFP-CM, in Fig. 3*E*). Together, these results suggest that BSR-K1 functions in the cytoplasm.

BSR-K1 Binds to *OsPAL1* mRNA in Rice. TPR-containing proteins have been reported to regulate mRNA metabolism (23–25). We hypothesized that BSR-K1, containing TPRs, may associate selectively with specific RNA transcripts. To address this, we performed two independent experiments of in vitro RNA immunoprecipitation (RIP) assays by separately coincubating GST and recombinant GST-BSR-K1 protein with rice total RNA (Fig. S5 *A* and *B*) and subsequently purifying GST, followed by high-throughput sequencing to identify BSR-K1–associated mRNAs. RNA electrophoresis analysis revealed that GST-BSR-K1, but not GST alone, is able to bind to RNA in vitro (Fig. S5*C*). By comparing the RNAs coprecipitated with GST-BSR-K1 (RIP) and GST (mock), we identified 82 and 110 RNA fragments from these two RIP assays, respectively, that were specifically and significantly coprecipitated by the GST-BSR-K1 protein (Dataset S3 *A* and *B*); 40 of the fragments were found in both assays (Dataset S3*C*). Interestingly, *OsPAL1* RNA fragments are highly represented in both RIP assays (Dataset S3*C*). Previous studies have shown up-regulation of *PAL1* genes, which results in enhanced immunity upon pathogen infection (26, 27). We then performed qRT-PCR to validate the enrichment of *OsPAL1* RNA in the

RIP precipitates (Fig. 4*A*). Further analysis showed that biotinylated *OsPAL1* RNA was able to pull down the full-length BSR-K1 (GST-BSR-K1$^{1–1,196\ aa}$) protein but not two truncated, nonfunctional BSR-K1 proteins, GST-BSR-K$^{1–105\ aa}$ and GST-BSR-K1$^{1–288\ aa}$ (Fig. 4*B*). Together, these results demonstrate direct binding of the BSR-K1 protein to *OsPAL1* mRNA in vitro.

We then generated transgenic plants carrying the native promoter-*3×HA-Bsr-k1*, which encodes HA-tagged BSR-K1 protein and complements the *bsr-k1* mutant (Fig. S5*D*). We detected and immunoprecipitated the 3×HA-BSR-K1 fusion protein using anti-HA antibody (Fig. S5 *E* and *F*). We then performed an in vivo RIP assay using transgenic and Kitaake plants. qRT-PCR analysis showed that the *OsPAL1* mRNA was pulled down by the 3×HA-BSR-K1 protein (Fig. 4*C*), confirming the binding of the BSR-K1 protein to *OsPAL1* mRNA in vivo.

BSR-K1 Regulates the *OsPAL1* mRNA Level Through Modulating the *OsPAL1* mRNA Turnover. We next tested whether the *OsPAL1* mRNA level is altered in *bsr-k1*. The results showed that *OsPAL1* mRNA accumulated to a higher level (~threefold) in *bsr-k1* than in Kitaake plants (Fig. 4*D*), indicating that BSR-K1 suppresses *OsPAL1* mRNA accumulation in Kitaake plants.

We then compared the turnover rate of *OsPAL1* mRNA in *bsr-k1* and Kitaake. We designed primers for qPCR to detect the 5′ end and 3′ end of *OsPAL1* mRNA, respectively (Fig. S6*A*), because mRNA degradation generally starts from the 3′ end, and thus the 5′-end/3′-end ratio represents its turnover rate (28). The reverse primers for each fragment were used to prime separate cDNA synthesis reactions (28). We found that Kitaake has a 5′-end/3′-end ratio approximately twice as high as *bsr-k1* (Fig. 4*E*), suggesting that the turnover rate of *OsPAL1* mRNA is compromised in *bsr-k1*. Together, these results indicate that BSR-K1 binds *OsPAL1* mRNA and promotes its turnover in Kitaake.

To determine whether the elevated *OsPAL1* mRNA level contributes to resistance to rice blast, we overexpressed the *OsPAL1* gene in a susceptible rice variety, TP309 (Fig. 4*F*), and performed blast inoculation. We found that the *OsPAL1* overexpression lines showed enhanced resistance to blast with lesion lengths significantly (three- to sevenfold) shorter than those observed for TP309 (Fig. 4 *G* and *H*), supporting the role of *OsPAL1* in *bsr-k1*–mediated resistance. However, KO of *OsPAL1* in *bsr-k1* or Kitaake plants did not compromise resistance to blast (Fig. 4 *I* and *J* and Fig. S6 *B*–*E*), suggesting that other *OsPAL* members may function redundantly and compensate for the loss of *OsPAL1*. In support, we also find that *bsr-k1* accumulates higher levels of *OsPAL1*–*OsPAL7* (especially *OsPAL1*–*OsPAL4*) mRNAs than Kitaake (Fig. 4*K*) and that BSR-K1 binds *OsPAL1*–*OsPAL7* mRNAs and facilitates their turnover in vivo (Fig. S6 *F*–*H*). For comparison, we also analyzed other defense-related genes, *Os11g0703900*, *Os05g0343400* (*WRKY53*), and *Os05g0293500*, detected in RIP sequencing (RIP-seq) (Dataset S3*C*). BSR-K1 showed very weak or no binding to these genes (Fig. S6*G*). Consistently, none of their mRNA turnover was remarkably repressed (Fig. S6*H*); their mRNAs did not significantly accumulate compared with *OsPAL1-7* in the *bsr-k1* mutant (Fig. 4*K*). Together, these results indicate that BSR-K1 preferentially promotes *OsPAL* mRNA turnover in rice plants and that loss of function of BSR-K1 (*bsr-k1*) results in mRNA accumulation of multiple *OsPAL* genes, leading to enhanced resistance in *bsr-k1*.

Plants Carrying Homozygous *bsr-k1* Alleles Exhibit Enhanced Resistance with No Major Yield Penalty. To assess the usefulness of the *bsr-k1* allele for rice blast control, we performed field trials in two rice-growing regions. Field one (Pujiang, Sichuan, China) was a field with high blast infection (29); as a control, field two (Lingshui, Hainan, China) had little or no *M. oryzae* present. We found that the *bsr-k1* plants displayed high levels of leaf and panicle resistance to *M. oryzae* in field one, whereas the Kitaake control plants succumbed to infection (Fig. 5*A* and Fig. S7).

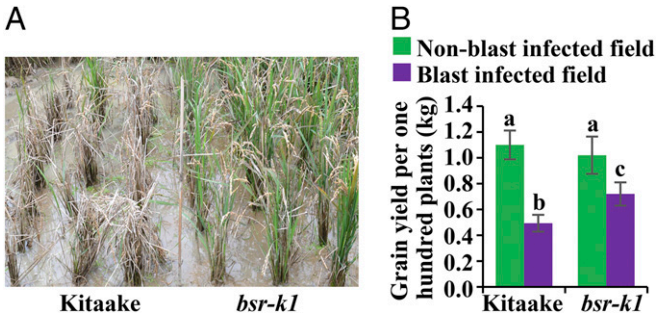

Fig. 5. Field trial of the *bsr-k1* rice line for blast resistance and yield property. (*A*) Field trial of *bsr-k1* and Kitaake plants on resistance to blast. Photographs were taken at the mature stage. (*B*) Evaluation of grain yield of *bsr-k1* and Kitaake plants in Lingshui and Pujiang. Grain yield was calculated as per 100 plants (mean ± SD, $n > 3$). Different letters above bars indicate different statistical groups ($P < 0.05$, Tukey's test).

We then evaluated the grain yield of *bsr-k1* plants and Kitaake control plants in the two fields. In field two, where no obvious blast infection occurred, the *bsr-k1* plants yielded a similar amount of grain as Kitaake plants (1.02 vs. 1.10 kg) (Fig. 5*B*). In contrast, in field one, where heavy blast infection occurred, the yield of *bsr-k1* plants was significantly higher than that of Kitaake plants (0.72 vs. 0.49 kg) (Fig. 5*B*). Furthermore, in three field tests at two locations, elite rice cultivars carrying *bsr-k1*, including Shuihui527$^{bsr\text{-}k1/bsr\text{-}k1}$, Minghui63$^{bsr\text{-}k1/bsr\text{-}k1}$, and Mianhui725$^{bsr\text{-}k1/bsr\text{-}k1}$ (Fig. S8), showed agronomic traits and yields similar to those of their parents, except for slightly lower yields of Shuhui527$^{bsr\text{-}k1/bsr\text{-}k1}$ and Minghui63$^{bsr\text{-}k1/bsr\text{-}k1}$ in one test (in Pujiang, 2016) (Dataset S4).

Discussion

We have demonstrated that loss of function of the *Bsr-k1* gene encoding a TPR-domain protein leads to enhanced resistance to all tested isolates of *M. oryzae* and *Xoo*. We conclude that the *bsr-k1* mutant clearly confers broad-spectrum disease resistance. None of the previously reported genes (7–15) conferring broad-spectrum resistance encodes proteins with RNA-binding activity. Thus, BSR-K1 represents a class of protein regulating a pathway leading to broad-spectrum resistance. Loss of functional BSR-K1 (*bsr-k1*) results in mRNA accumulation of multiple *OsPAL* (*OsPAL1*–*OsPAL7*) genes (Fig. 4*K*). We hypothesize that BSR-K1 promotes mRNA degradation of these *OsPAL* genes and that loss of function of BSR-K1 results in lower turnover of their mRNAs, leading to mRNA accumulation.

Previous studies have shown that the expression of *PAL1* genes is required for the biosynthesis of secondary metabolites, including lignin and SA, a phytohormone associated with defense against biotrophic pathogens (27). Our results show that *bsr-k1* accumulates more lignin, but not total SA (Fig. S9 *A* and *B*), despite the elevation of defense-related genes such as *OsPR1a* in *bsr-k1* (Fig. 1*E*). Consistently, the lignin content also accumulates in *OsPAL1* overexpression plants (Fig. S9*C*) that exhibit enhanced resistance to rice blast (Fig. 4 *F*–*H*), but the SA content remains unchanged (Fig. S9*D*). These results indicate that higher expression levels of *OsPAL* genes increase the biosynthesis of lignin, instead of SA, and resistance to pathogens in the *bsr-k1* mutant. However, how the elevation of lignin content is associated with the activation of defense genes remains unknown.

TPR-containing proteins are involved in the regulation of RNA metabolism in various organisms (23–25). Our results demonstrate that the BSR-K1 protein regulates mRNA turnover of multiple *OsPAL* genes (Fig. 4*E* and Fig. S6*H*). Thus, BSR-K1 regulates plant immunity through a mechanism different from those of

previously identified RNA-binding proteins (30–32). For example, *Arabidopsis* MOS2 is required for proper splicing of *SNC1*, and loss of MOS2 function results in suppressing the autoimmune responses in *snc1* (30). Bean PRP-BP participates in the elicitor-induced destabilization of *PvPRP1* mRNA, which encodes a cell wall-strengthening protein, implicating PRP-BP in plant defense (31). Human HuR regulates the splicing of *Dlst* mRNA, encoding a subunit of the 2-oxoglutarate dehydrogenase (a-KGDH) complex; absence of HuR results in large amounts of reactive oxygen species and B cell death (32).

In rice, it has been reported that TPR proteins mainly act as interaction scaffolds in the formation of multiprotein complexes involved in the immune response, such as in the defensome of chitin-induced immunity (33). This defensome complex includes two TPR proteins, OsSGT1 and OsSti1a, which associate with the HSP90 immune complex to regulate chitin-triggered immunity and resistance against rice blast fungus (33). In contrast, BSR-K1 does not directly interact with the rice defensome complex (Fig. S10*A*). Thus, the action of the BSR-K1 TPR protein represents a mechanism leading to immunity regulated through interaction with mRNA. Because the TPR motifs are highly conserved in diverse organisms (34), we hypothesize that TPR proteins, especially those sharing high homologies to BSR-K1, including *Arabidopsis* AtSKI3 (Fig. S10*B*), may also be involved in regulating immune responses via a similar mechanism.

In practice, most breeding programs rely on dominant resistance (*R*) genes (35), which often confer race-specific resistance and are overcome by the evolution of new pathogen races within a few years (36). Although a number of genes or QTLs for broad-spectrum and durable resistance have been identified (7–15), the tight linkage to undesirable agricultural traits has often hindered breeding. The *bsr-k1* mutant confers broad-spectrum resistance with no major penalty on main agronomic traits (Fig. 1*F* and Fig. S1*B*). The moderately elevated activation of defense-related genes in *bsr-k1* (Fig. 1*E*) is sufficient to suppress pathogen attack, similar to the putative characteristics of *pi21*-mediated resistance (10). Indeed, the *bsr-k1* allele strikingly improves rice resistance in Kitaake in a naturally blast-diseased field compared with the wild-type *Bsr-k1* allele (Fig. 5*A* and Fig. S7). Three field tests of elite rice cultivars suggest that the *bsr-k1* allele does not carry a major penalty affecting main agronomic traits or yield (Dataset S4), making it a good candidate for rice breeding.

Materials and Methods

Rice blast and *Xoo* infections and disease assessments were performed as described (21, 22, 29). Purified recombinant proteins from *Escherichia coli* were used for in vitro RIP assays and RNA pulldown assays. Immunoprecipitated recombinant proteins from transgenic rice were used for in vivo RIP assays. In vitro RIP assays and in vivo RIP assays were performed as described (37). The RNA pulldown assay was performed using the Pierce Magnetic RNA-Protein Pull-Down Kit following the manufacturer's instructions (Thermo Scientific). Determination of mRNA turnover was performed as described (28). The blast isolates used to identify Kitaake-compatible blast isolates are listed in Dataset S5. The primers used for qRT-PCR are listed in Dataset S6. All other materials and details of experimental methods can be found in *SI Materials and Methods*.

ACKNOWLEDGMENTS. X.C. was supported by National Science Foundation of China (NSFC) Grants 31171622 and 31571994, National Key Research and Development Program of China Grant 2016YFD0100600, Transgenic Projects from the Chinese Ministry of Agriculture (TPCMA) Grant 2014ZX0800903B, Program for New Century Excellent Talents in University from the Ministry of Education in China Grant NECT-13-0920, and "Hundred Talents Plan" Foundation Youth Foundation Grant 13QNJJ0076. J.Y. was supported by NSFC Grant 31601290. M.C. and P.C.R. were supported by National Science Foundation Grant PGRP IOS 1237975, NIH Grant GM59962, and US Department of Agriculture National Institute of Food and Agriculture Grant 2017-67013-26590. Jing Wang was supported by NSFC Grant 31401351. W.L. was supported by NSFC Grant 31501627, and B.M. was supported by TPCMA Grant 2016ZX08001002.

1. Azizi P, et al. (2016) Toward understanding of rice innate immunity against *Magnaporthe oryzae*. *Crit Rev Biotechnol* 36:165–174.
2. Talbot NJ (2003) On the trail of a cereal killer: Exploring the biology of *Magnaporthe grisea*. *Annu Rev Microbiol* 57:177–202.
3. Hu KM, Qiu DY, Shen XL, Li XH, Wang SP (2008) Isolation and manipulation of quantitative trait loci for disease resistance in rice using a candidate gene approach. *Mol Plant* 1:786–793.
4. Miah G, et al. (2013) Blast resistance in rice: A review of conventional breeding to molecular approaches. *Mol Biol Rep* 40:2369–2388.
5. Kou Y, Wang S (2012) Toward an understanding of the molecular basis of quantitative disease resistance in rice. *J Biotechnol* 159:283–290.
6. Kou Y, Wang S (2010) Broad-spectrum and durability: Understanding of quantitative disease resistance. *Curr Opin Plant Biol* 13:181–185.
7. Xiao S, et al. (2001) Broad-spectrum mildew resistance in *Arabidopsis thaliana* mediated by *RPW8*. *Science* 291:118–120.
8. Song WY, et al. (1995) A receptor kinase-like protein encoded by the rice disease resistance gene, *Xa21*. *Science* 270:1804–1806.
9. Wang Q, et al. (2014) *STV11* encodes a sulphotransferase and confers durable resistance to rice stripe virus. *Nat Commun* 5:4768.
10. Fukuoka S, et al. (2009) Loss of function of a proline-containing protein confers durable disease resistance in rice. *Science* 325:998–1001.
11. Deng Y, et al. (2017) Epigenetic regulation of antagonistic receptors confers rice blast resistance with yield balance. *Science* 355:962–965.
12. Li W, et al. (2017) A natural allele of a transcription factor in rice confers broad-spectrum blast resistance. *Cell* 170:114–126.e15.
13. Krattinger SG, et al. (2009) A putative ABC transporter confers durable resistance to multiple fungal pathogens in wheat. *Science* 323:1360–1363.
14. Fu D, et al. (2009) A kinase-START gene confers temperature-dependent resistance to wheat stripe rust. *Science* 323:1357–1360.
15. Büschges R, et al. (1997) The barley *Mlo* gene: A novel control element of plant pathogen resistance. *Cell* 88:695–705.
16. Wang W, Wen Y, Berkey R, Xiao S (2009) Specific targeting of the *Arabidopsis* resistance protein RPW8.2 to the interfacial membrane encasing the fungal Haustorium renders broad-spectrum resistance to powdery mildew. *Plant Cell* 21:2898–2913.
17. Chen X, Ronald PC (2011) Innate immunity in rice. *Trends Plant Sci* 16:451–459.
18. Gou JY, et al. (2015) Wheat stripe rust resistance protein WKS1 reduces the ability of the thylakoid-associated ascorbate peroxidase to detoxify reactive oxygen species. *Plant Cell* 27:1755–1770.
19. Chen H, Iqbal M, Yang RC, Spaner D (2016) Effect of *Lr34/Yr18* on agronomic and quality traits in a spring wheat mapping population and implications for breeding. *Mol Breed* 36:53.
20. Piffanelli P, et al. (2002) The barley MLO modulator of defense and cell death is responsive to biotic and abiotic stress stimuli. *Plant Physiol* 129:1076–1085.
21. Park CH, et al. (2012) The *Magnaporthe oryzae* effector AvrPiz-t targets the RING E3 ubiquitin ligase APIP6 to suppress pathogen-associated molecular pattern-triggered immunity in rice. *Plant Cell* 24:4748–4762.
22. Han X, et al. (2014) Quantitative trait Loci mapping for bacterial blight resistance in rice using bulked segregant analysis. *Int J Mol Sci* 15:11847–11861.
23. Goebl M, Yanagida M (1991) The TPR snap helix: A novel protein repeat motif from mitosis to transcription. *Trends Biochem Sci* 16:173–177.
24. Sane AP, Stein B, Westhoff P (2005) The nuclear gene *HCF107* encodes a membrane-associated R-TPR (RNA tetratricopeptide repeat)-containing protein involved in expression of the plastidial *psbH* gene in *Arabidopsis*. *Plant J* 42:720–730.
25. Izumiyama T, Minoshima S, Yoshida T, Shimizu N (2012) A novel big protein TPRBK possessing 25 units of TPR motif is essential for the progress of mitosis and cytokinesis. *Gene* 511:202–217.
26. Kim DS, Hwang BK (2014) An important role of the pepper phenylalanine ammonia-lyase gene (*PAL1*) in salicylic acid-dependent signalling of the defence response to microbial pathogens. *J Exp Bot* 65:2295–2306.
27. Duan L, Liu H, Li X, Xiao J, Wang S (2014) Multiple phytohormones and phytoalexins are involved in disease resistance to *Magnaporthe oryzae* invaded from roots in rice. *Physiol Plant* 152:486–500.
28. Dorcey E, et al. (2012) Context-dependent dual role of SKI8 homologs in mRNA synthesis and turnover. *PLoS Genet* 8:e1002652.
29. Ye HL, et al. (2010) Study on control effects of rice mixture on rice blast in different ecological zones. *Xi Nan Nong Ye Xue Bao* 23:1510–1514.
30. Copeland C, Xu S, Qi Y, Li X (2013) MOS2 has redundant function with its homolog MOS2H and is required for proper splicing of *SNC1*. *Plant Signal Behav* 8:e25372.
31. Zhang S, Mehdy MC (1994) Binding of a 50-kD protein to a U-rich sequence in an mRNA encoding a proline-rich protein that is destabilized by fungal elicitor. *Plant Cell* 6:135–145.
32. Diaz-Muñoz MD, et al. (2015) The RNA-binding protein HuR is essential for the B cell antibody response. *Nat Immunol* 16:415–425.
33. Chen L, et al. (2010) The Hop/Sti1-Hsp90 chaperone complex facilitates the maturation and transport of a PAMP receptor in rice innate immunity. *Cell Host Microbe* 7:185–196.
34. Lamb JR, Tugendreich S, Hieter P (1995) Tetratrico peptide repeat interactions: To TPR or not to TPR? *Trends Biochem Sci* 20:257–259.
35. Pavan S, Jacobsen E, Visser RGF, Bai Y (2010) Loss of susceptibility as a novel breeding strategy for durable and broad-spectrum resistance. *Mol Breed* 25:1–12.
36. Panstruga R, Dodds PN (2009) Terrific protein traffic: The mystery of effector protein delivery by filamentous plant pathogens. *Science* 324:748–750.
37. Xing D, Wang Y, Hamilton M, Ben-Hur A, Reddy AS (2015) Transcriptome-wide identification of RNA targets of *Arabidopsis* SERINE/ARGININE-RICH45 uncovers the unexpected roles of this RNA binding protein in RNA processing. *Plant Cell* 27:3294–3308.